

*Precipitation changes in the  
Mediterranean basin during the Holocene  
from terrestrial and marine pollen records:  
a model–data comparison*

Article

Published Version

Creative Commons: Attribution 3.0 (CC-BY)

Discussion paper under review

Peyron, O., Combourieu-Nebout, N., Brayshaw, D. ORCID: <https://orcid.org/0000-0002-3927-4362>, Goring, S., Andrieu-Ponel, V., Desprat, S., Fletcher, W., Gambin, B., Ioakim, C., Joannin, S., Kotthoff, U., Kouli, K., Montade, V., Pross, J., Sadori, L. and Magny, M. (2017) Precipitation changes in the Mediterranean basin during the Holocene from terrestrial and marine pollen records: a model–data comparison. *Climate of the Past*, 13 (3). pp. 249-265. ISSN 1814-9324 doi: <https://doi.org/10.5194/cp-2016-65> Available at <https://centaur.reading.ac.uk/66127/>

It is advisable to refer to the publisher's version if you intend to cite from the work. See [Guidance on citing](#).

Published version at: <http://dx.doi.org/10.5194/cp-2016-65>

To link to this article DOI: <http://dx.doi.org/10.5194/cp-2016-65>

Publisher: Copernicus Publications on behalf of the European Geosciences Union

All outputs in CentAUR are protected by Intellectual Property Rights law, including copyright law. Copyright and IPR is retained by the creators or other

copyright holders. Terms and conditions for use of this material are defined in the [End User Agreement](#).

[www.reading.ac.uk/centaur](http://www.reading.ac.uk/centaur)

## **CentAUR**

Central Archive at the University of Reading

Reading's research outputs online



1 **The climate of the Mediterranean basin during the**  
2 **Holocene from terrestrial and marine pollen records: A**  
3 **model/data comparison**

4  
5 **Odile Peyron<sup>1</sup>, Nathalie Combourieu-Nebout<sup>2</sup>, David Brayshaw<sup>3</sup>, Simon**  
6 **Goring<sup>4</sup>, Valérie Andrieu-Ponel<sup>5</sup>, Stéphanie Desprat<sup>6,7</sup>, Will Fletcher<sup>8</sup>, Belinda**  
7 **Gambin<sup>9</sup>, Chryssanthi Ioakim<sup>10</sup>, Sébastien Joannin<sup>1</sup>, Ulrich Kotthoff<sup>11</sup>, Katerina**  
8 **Kouli<sup>12</sup>, Vincent Montade<sup>1</sup>, Jörg Pross<sup>13</sup>, Laura Sadori<sup>14</sup>, Michel Magny<sup>15</sup>**

9 [1] Institut des Sciences de l'Evolution (ISEM), Université de Montpellier, France

10 [2] UMR 7194 MNHN, Institut de Paléontologie Humaine 1, Paris, France

11 [3] University of Reading, Department of Meteorology, United Kingdom

12 [4] Department of Geography, Univ. of Wisconsin-Madison, Wisconsin, USA

13 [5] Institut Méditerranéen de Biodiversité et d'Ecologie marine et continentale (IMBE), Aix Marseille  
14 Université, Aix-en-Provence, France

15 [6] EPHE, PSL Research University, Laboratoire Paléoclimatologie et Paléoenvironnements Marins,  
16 Pessac, France

17 [7] Univ. Bordeaux, EPOC UMR 5805, Pessac, France

18 [8] Geography, School of Environment, Education and Development, University of Manchester, United  
19 Kingdom

20 [9] Institute of Earth Systems, University of Malta, Malta

21 [10] Institute of Geology and Mineral Exploration, Athens, Greece

22 [11] Center for Natural History and Institute of Geology, Hamburg University, Hamburg, Germany

23 [12] Department of Geology and Geoenvironment, National and Kapodistrian University of Athens, Greece

24 [13] Paleoenvironmental Dynamics Group, Institute of Earth Sciences, Heidelberg University, Germany

25 [14] Dipartimento di Biologia Ambientale, Università di Roma "La Sapienza", Roma, Italy

26 [15] UMR 6249 Chrono-Environnement, Université de Franche-Comté, Besançon, France

27 Correspondence to: O. Peyron ([odile.peyron@univ-montp2.fr](mailto:odile.peyron@univ-montp2.fr))



28 Abstract

29 Climate evolution of the Mediterranean region during the Holocene exhibits strong spatial and  
30 temporal variability. The spatial differentiation and temporal variability, as evident from  
31 different climate proxy datasets, has remained notoriously difficult for models to reproduce. In  
32 light of this complexity, we examine the previously described evidence for (i) opposing  
33 northern and southern precipitation regimes during the Holocene across the Mediterranean  
34 basin, and (ii) an east-to-west precipitation gradient or dipole during the early Holocene, from  
35 a wet eastern Mediterranean to dry western Mediterranean. Using quantitative climate  
36 information from marine and terrestrial pollen archives, we focus on two key time intervals, the  
37 early to mid-Holocene (8000 to 6000 cal yrs BP) and the late Holocene (4000 to 2000 yrs BP),  
38 in order to test the above mentioned hypotheses on a Mediterranean-wide scale. Palynologically  
39 derived climate information is compared with the output of regional-scale climate-model  
40 simulations for the same time intervals.

41 Quantitative pollen-based precipitation estimates were generated along a longitudinal gradient  
42 from the Alboran (West) to the Aegean Sea (East); they are derived from terrestrial pollen  
43 records from Greece, Italy and Malta as well as from pollen records obtained from marine cores.  
44 Because seasonality represents a key parameter in Mediterranean climates, special attention  
45 was given to the reconstruction of season-specific climate information, notably summer and  
46 winter precipitation. The reconstructed climatic trends corroborate a previously described  
47 north-south partition of precipitation regimes during the Holocene. During the early Holocene,  
48 relatively wet conditions occurred in the south-central and eastern Mediterranean region, while  
49 drier conditions prevailed from 45°N northwards. These patterns reversed during the late  
50 Holocene, with a wetter northern Mediterranean region and drier conditions in the east and  
51 south. More sites from the northern part of the Mediterranean basin are needed to further  
52 substantiate these observations. With regard to the existence of a west-east precipitation dipole  
53 during the Holocene, our pollen-based climate data show that the strength of this dipole is  
54 strongly linked to the seasonal parameter reconstructed: Early Holocene summers show a clear  
55 east-to-west gradient, with summer precipitation having been highest in the central and eastern  
56 Mediterranean and lowest over the western Mediterranean. In contrast, winter precipitation  
57 signals are less spatially coherent. A general drying trend occurred from the early to the late  
58 Holocene; particularly in the central and eastern Mediterranean. However, summer  
59 precipitation in the east remained above modern values, even during the late Holocene interval.



60 Pollen-inferred precipitation estimates were compared to regional-scale climate modelling  
61 simulations based on the HadAM3 GCM coupled to the dynamic HadSM3 and the high-  
62 resolution regional HadRM3 models. Climate model outputs and pollen-inferred precipitation  
63 estimates show remarkably good overall correspondence, although many simulated patterns are  
64 of marginal statistical significance. Nevertheless, models weakly support an east to west  
65 division in summer precipitation and there are suggestions that the eastern Mediterranean  
66 experienced wetter summer and winter conditions during the early Holocene and wetter  
67 summer conditions during the late Holocene. The extent to which summer monsoonal  
68 precipitation may have existed in the southern and eastern Mediterranean during the mid-  
69 Holocene remains an outstanding question; our model, consistent with other global models,  
70 does not suggest an extension of the African monsoon into the Mediterranean. Given the  
71 difficulty in modelling future climate change in Southern Europe, more simulations based on  
72 high resolution global models and very high resolution regional downscaling, perhaps even  
73 including transient simulations, are required to fully understand the patterns of change in winter  
74 and summer circulation patterns over the Mediterranean region.

75  
76



## 77 1 Introduction

78 The Mediterranean region is particularly sensitive to climate change due to its position within  
79 the confluence of arid North African (i.e., subtropically influenced) and temperate/humid  
80 European (i.e., mid-latitude) climates (Lionello, 2012). Palaeoclimatic proxies, including  
81 stable isotopes, lipid biomarkers, palynological data and lake-levels, have shown that the  
82 Mediterranean region experienced climatic conditions that varied spatially and temporally  
83 throughout the Holocene (e.g. Bar-Matthews and Ayalon, 2011; Luterbacher et al., 2012;  
84 Lionello, 2012; Triantaphyllou et al., 2014, 2016; Mauri et al., 2015; De Santis and Caldara  
85 2015; Sadori et al., 2016a) and well before (eg. Sadori et al., 2016b). Clear spatial climate  
86 patterns have been identified from east to west and from north to south within the basin (e.g.  
87 Zanchetta et al., 2007 ; Magny et al., 2009b, 2011, 2013; Zhorniyak et al., 2011 ; Sadori et al.,  
88 2013; Fletcher et al., 2013 ). Lake-level reconstructions from Italy suggest contrasting patterns  
89 of palaeohydrological changes for the central Mediterranean during the Holocene (Magny et  
90 al., 2012, 2013). Specifically, lake level maxima occurred south of approximately 40°N in the  
91 early to mid-Holocene, while lakes north of 40°N recorded minima. This pattern was reversed  
92 at around 4500 cal yrs BP.

93 Quantitative pollen-based precipitation reconstructions from sites in northern Italy indicate  
94 humid winters and dry summers during the early to mid-Holocene, whereas southern Italy was  
95 characterised by humid winters and summers; the N-S pattern reverses in the late Holocene,  
96 with drier conditions at southern sites and wet conditions at northern sites. These findings  
97 support a North–South partition for the central Mediterranean with regards to precipitation, and  
98 also confirm that precipitation seasonality is a key parameter in the evolution of Mediterranean  
99 climates (Peyron et al., 2013). The pattern of shifting N-S precipitation regimes has also been  
100 identified for the Aegean Sea (Peyron et al., 2013). Taken together, the evidence from pollen  
101 data and from other proxies covering the Mediterranean region suggest a climate response that  
102 can be linked to a combination of orbital, ice-sheet and solar forcings (Magny et al., 2013).

103 An east-west pattern of climatic change during the Holocene is also observed in the  
104 Mediterranean region (e.g., Combourieu Nebout et al., 1998; Geraga et al., 2010; Colmenero-  
105 Hildago et al., 2002; Kotthoff et al., 2008; Dormoy et al., 2009; Finne et al., 2011; Roberts et  
106 al., 2011, 2012; Luterbacher et al., 2012; Guiot and Kaniewski, 2015). A gradient of  
107 precipitation or an east-west division during the Holocene is suggested by marine pollen records  
108 (Dormoy et al., 2009), lake-level reconstructions (Magny et al., 2013) and speleothem isotopes



109 (Roberts et al. 2011); the east-west pattern of change has also been corroborated through a  
110 Bayesian inverse modelling approach (Guiot and Kaniewski, 2015)

111 This study aims to reconstruct and evaluate N-S and W-E climate gradients for the  
112 Mediterranean basin, over two key periods in the Holocene, 8000-6000 cal yrs BP, and 4000-  
113 2000 cal yrs BP. We estimate the magnitude of precipitation changes and reconstruct climatic  
114 trends across the Mediterranean using both terrestrial and marine high-resolution pollen  
115 records. Precipitation is estimated using the Modern Analogue Technique (Guiot 1990) for five  
116 pollen records from Greece, Italy and Malta, and for eight marine pollen records along a  
117 longitudinal gradient from the Alboran Sea to the Aegean Sea. Because precipitation  
118 seasonality is a key parameter of change during the Holocene in the Mediterranean (Rohling et  
119 al., 2002; Peyron et al., 2011, Mauri et al., 2015), the quantitative climate estimates focus on  
120 reconstructing changes in summer and winter precipitation.

121 Paleoclimate proxy data are essential benchmarks for model intercomparison and validation  
122 (e.g., Morrill et al., 2012; Heiri et al., 2014). This holds particularly true considering that  
123 previous model-data intercomparisons have revealed substantial difficulties for GCMs in  
124 simulating key aspects of Holocene climate (Hargreaves et al., 2013) for Europe (Mauri et al.,  
125 2014), and notably for Southern Europe (Davis and Brewer, 2009; Mauri et al., 2015). We aim  
126 to identify and quantify the spatio-temporal climate patterns in the Mediterranean Basin for two  
127 key intervals of the Holocene (8000–6000 and 4000–2000 cal yrs BP) based on terrestrial and  
128 marine high-resolution pollen records. Spatially, we focus on transects across the  
129 Mediterranean basin from north to south and from west to east. Because precipitation  
130 seasonality is a key parameter of Holocene climate change in the Mediterranean (Rohling et al.,  
131 2002; Peyron et al., 2011, Mauri et al., 2015), our quantitative climate estimates focus on  
132 summer and winter precipitation. Finally, we compare our pollen-inferred climate patterns with  
133 regional-scale climate model simulations (Brayshaw et al., 2011a) in order to critically assess  
134 the potential of the model set-up used to reproduce Holocene climate variability.

135

## 136 **2 Sites, pollen records, and models**

137 The Mediterranean region is at the confluence of continental and tropical air masses.  
138 Specifically, the central and eastern Mediterranean is influenced by monsoonal systems, while  
139 the north-western Mediterranean is under stronger influence from mid-latitude climate regimes  
140 (Lionello et al., 2006). Mediterranean winter climates are mostly dominated by storm systems



141 originating over the Atlantic. In the western Mediterranean, precipitation is predominantly  
142 affected by the North Atlantic Oscillation (NAO), while several systems interact to control  
143 precipitation over the northern and eastern Mediterranean (Giorgi and Lionello, 2008).  
144 Mediterranean summer climates are dominated by descending high pressure systems that lead  
145 to dry/hot conditions, particularly over the southern Mediterranean where climate variability is  
146 strongly influenced by African and Asian monsoons (Alpert et al., 2006) with strong  
147 geopotential blocking anomalies over central Europe (Giorgi and Lionello, 2008; Trigo et al.,  
148 2006).

149 The palynological component of our study combines results from five terrestrial and eight  
150 marine pollen records to provide broad coverage of the Mediterranean basin (Figure 1, Table  
151 1). The terrestrial sequences comprise pollen records from lakes along a latitudinal gradient  
152 from northern Italy (Lakes Ledro and Accesa) to Sicily (Lake Pergusa), one pollen record from  
153 Malta (Burmarrad) and one pollen record from Greece (Tenaghi Philippon). The marine pollen  
154 sequences are situated along a longitudinal gradient across the Mediterranean Sea; from the  
155 Alboran Sea (ODP Site 976 and core MD95-2043), Siculo-Tunisian strait (core MD04-2797),  
156 Adriatic Sea (core MD90-917), and Aegean Sea (cores SL152, MNB-3, NS14, HCM2/22). For  
157 each record we used the chronologies as reported in the original publications (see Table 1 for  
158 references).

159 Climate reconstructions for summer and winter precipitation (Figs. 2, 3) inferred from the  
160 terrestrial sequences and marine pollen records were performed using the Modern Analogue  
161 Technique (MAT; Guiot, 1990). The MAT compares fossil pollen assemblages to modern  
162 pollen assemblages with known climate parameters. The MAT is calibrated using an expanded  
163 surface pollen dataset with more than 3600 surface pollen samples from various European  
164 ecosystems (Peyron et al., 2013). In this dataset, 2200 samples are from the Mediterranean  
165 region, and the results shows that the analogues selected here are limited to the Mediterranean  
166 basin. Since the MAT use the distance structure of the data and essentially perform local fitting  
167 of the climate parameter (as the mean of  $n$ -closest sites) they may be less susceptible to  
168 increased noise in the data set, and less likely to report spurious values than others methods (for  
169 more details on the method, see Peyron et al., 2011). *Pinus* is overrepresented in marine pollen  
170 samples (Heusser and Balsam, 1977; Naughton et al., 2007), and as such *Pinus* pollen was  
171 removed from the assemblages for the calibration of marine records using MAT.

172 Climate model simulations focused on regional-scale climate modelling simulations based on  
173 the HadAM3 GCM and the high-resolution regional HadRM3 models. Climate simulations are





174 described fully in Brayshaw et al. (2010, 2011a, b). The HadAM3 global atmospheric model  
175 (resolution 2.5° latitude x 3.75° longitude, 19 vertical levels; Pope et al., 2000) is coupled to a  
176 slab ocean (Hewitt et al., 2001) and used to perform a series of time slice experiments. Each  
177 time-slice simulation corresponds to 20 model years after spin up (40 model years for pre-  
178 industrial). The time slices correspond to “preindustrial”, 2000 cal BP, 4000 cal BP, 6000 cal  
179 BP and 8000 cal BP conditions, and are forced with appropriate insolation (associated with  
180 changes in the Earth’s orbit), and atmospheric CO<sub>2</sub> and CH<sub>4</sub> concentrations. The heat fluxes in  
181 the ocean are held fixed (and there is no sea-level change) using values taken from a pre-  
182 industrial control run, but sea-surface temperatures are allowed to evolve freely. The coarse  
183 global output from the model for each time slice is downscaled over the Mediterranean region  
184 using HadRM3 (i.e. a limited area version of the same atmospheric model; resolution 0.44° x  
185 0.44°, with 19 vertical levels). Unlike the global model, HadRM3 is not coupled to an ocean  
186 model; instead, sea-surface temperatures are derived directly from the HadSM3 output.

187 To aid interpretability (and to increase the signal-to-noise ratio), time slice experiments are  
188 grouped into “late Holocene” (4000 BP and 2000 cal yrs BP) and “mid Holocene” (8000 BP  
189 and 6000 cal yrs BP) experiments. Changes in climate are expressed as differences with respect  
190 to the preindustrial control run and statistical significance is assessed with the Wilcoxon-Mann-  
191 Whitney significance test (Wilks, 1995).

192

### 193 **3 Results and Discussion**

194

#### 195 *A North-South precipitation pattern?*

196 Proxy evidence shows contrasting patterns of palaeohydrological changes in the central  
197 Mediterranean. The early-to-mid-Holocene was characterized by lake-level and precipitation  
198 maxima south of around 40°N. At the same time, northern Italy experienced precipitation and  
199 lake-levels minima. This pattern reverses after 4500 cal yrs BP (Magny et al., 2012b; Peyron et  
200 al., 2013). Other proxies suggest contrasting North-South hydrological patterns across the  
201 Mediterranean (Magny et al., 2013). We focus on two key time periods, the early to mid-  
202 Holocene (8000-6000 cal yrs BP), and the late Holocene (4000-2000 cal yrs BP) in order to test  
203 this hypothesis across the Mediterranean, and to compare the results with regional climate  
204 simulations for the same time periods.

205 Early to mid-Holocene (8000 to 6000 cal yrs BP)



206 Climatic trends reconstructed from both marine and terrestrial pollen records seem to  
207 corroborate the hypothesis of a north-south division in precipitation regimes during the  
208 Holocene (Fig 2a). Our results confirm that northern Italy was characterized by drier conditions  
209 (relative to modern) while the south-central Mediterranean experienced more annual, winter  
210 and summer precipitation during the early to mid-Holocene (Fig. 2a). Only Burmarrad (Malta)  
211 shows drier conditions in the early to mid-Holocene (Fig 2a), although summer precipitation  
212 reconstructions are marginally higher than modern at the site. Wetter summer conditions in the  
213 Aegean Sea suggest a regional, wetter, climate signal over the central and eastern  
214 Mediterranean. Winter precipitation in the Aegean Sea is less spatially coherent, with dry  
215 conditions in the North Aegean Sea and wet or near-modern conditions in the Southern Aegean  
216 Sea (Fig. 2a).

217 Precipitation reconstructions are particularly important for this region given that precipitation  
218 rather than temperature represents the dominant controlling factor on Mediterranean  
219 environmental system during the early to mid-Holocene (Renssen et al., 2012). Pollen and non-  
220 pollen proxies, including marine and terrestrial biomarkers (terrestrial n-alkanes), indicate  
221 humid mid-Holocene conditions in the Aegean Sea (Triantaphyllou et al., 2014, 2016). Results  
222 within the Aegean support the pollen-based reconstructions, but non-pollen proxy data are still  
223 lacking at the basin scale in the Mediterranean, limiting our ability to undertake independent  
224 evaluation of precipitation reconstructions.

225 Very few large-scale climate reconstruction of precipitation exist for the whole Holocene  
226 (Bartlein et al., 2011; Mauri et al., 2014; Guiot and Kaniewski, 2015, Tarroso et al., 2016) and,  
227 even at local scales, pollen-inferred reconstructions of seasonal precipitation are very rare (Wu  
228 et al., 2007; Peyron et al., 2011, 2013; Combourieu-Nebout et al., 2013, Nourelbait et al., 2016).  
229 Several studies focused on the 6000 cal years BP period: Wu et al. (2007) reconstruct regional  
230 seasonal and annual precipitation and suggest that precipitation did not differ significantly from  
231 modern conditions across the Mediterranean; however, scaling issues render it difficult to  
232 compare their results with the reconstructions presented here. Cheddadi et al. (1997) reconstruct  
233 wetter-than-modern conditions at 6000 yrs cal BP in southern Europe; however, their study uses  
234 only one record from Italy and measures the moisture availability index which is not directly  
235 comparable to precipitation *sensu stricto* since it integrates temperature and precipitation. At  
236 6000 yrs cal BP, Bartlein et al. (2011) reconstruct Mediterranean precipitation at values between  
237 100 and 500 mm higher than modern. Mauri et al. (2015), in an updated version of Davis et al.  
238 (2003), provide a quantitative climate reconstructions comparable to the seasonal precipitation



239 reconstructions presented here. Compared to Davis et al. (2003), which focused on Holocene  
240 pollen-based temperature reconstructions for Europe, Mauri et al. (2015) have a broader set of  
241 sites and present reconstructed seasonal and annual precipitation. Mauri et al. (2015) results differ  
242 from the current study in using MAT with plant functional type scores and in producing gridded  
243 climate maps (Fig. 2b). Mauri et al. (2015) show wetter summers in Southern Europe (Greece  
244 and Italy) with a precipitation maximum between 8000 and 6000 cal yrs BP (Fig 2b), where  
245 precipitation was ~20 mm/month higher than modern. As in our reconstruction, precipitation  
246 changes in the winter were small and not significantly different from present-day conditions (Fig  
247 2b). Our reconstructions are in good agreement with Mauri et al. (2015), with summer (and  
248 annual) precipitation lower than modern over the northern Mediterranean region and wetter  
249 summer conditions over much of the south-central Mediterranean, while winter conditions  
250 appear to be similar to modern values. Mauri et al. (2015) results inferred from terrestrial pollen  
251 records and the climatic trends reconstructed here from marine and terrestrial pollen records  
252 seems to corroborate the hypothesis of a north-south division in precipitation regimes during the  
253 Early to Mid-Holocene in central Mediterranean.

254

#### 255 Late Holocene (4000 to 2000 cal yrs BP)

256 Late Holocene reconstructions of winter and summer precipitation indicate that the pattern  
257 established during the early Holocene was reversed by 4000 cal yrs BP, with higher  
258 precipitation in northern Italy and lower precipitation in southern Italy and Malta (Fig. 2a).  
259 Annual precipitation reconstructions suggest drying relative to the early Holocene, with modern  
260 conditions in northern Italy, and drier than modern conditions in central and southern Italy  
261 during most of the Late Holocene. Reconstructions for the Aegean Sea indicate higher summer  
262 and annual precipitation (Fig. 2b). Winter conditions reverse the early to mid-Holocene trend,  
263 with wetter conditions in the northern Aegean Sea and drier conditions in the southern Aegean  
264 Sea (Fig. 2b). Our reconstructions from all sites show a good fit with Mauri et al. (2015), except  
265 for the Alboran Sea where we reconstruct relatively wet conditions, whereas Mauri et al. (2015)  
266 reconstruct dry conditions (Fig. 2b). Our reconstruction of summer precipitation is very similar  
267 to Mauri et al. (2015) for Greece and the Aegean Sea where wet conditions are reported (Fig.  
268 2b).

269



270 *An East-West precipitation pattern?*

271 An East to West precipitation gradient, or an East-West division during the Holocene has been  
272 suggested for the Mediterranean from pollen data and lakes isotopes (Dormoy et al., 2009;  
273 Roberts et al., 2011; Guiot and Kaniewski, 2015). However, lake-levels and other hydrological  
274 proxies around the Mediterranean Basin do not clearly support this hypothesis and rather show  
275 contrasting hydrological patterns south and north of 40°N particularly during the Holocene  
276 climatic optimum (Magny et al., 2013).

277 Early to mid-Holocene (8000 to 6000 cal yrs BP)

278 The annual precipitation and seasonal precipitation signals appear to conflict in the early  
279 Holocene (Fig. 2a). The pollen-inferred annual precipitation indicates unambiguously wetter  
280 than today conditions south of 45°N in the western, central and eastern Mediterranean, except  
281 for Malta (Fig. 2a). Winter conditions show less spatial coherence, although the western basin  
282 appears to have experienced higher precipitation than modern, while drier conditions exist in  
283 the east (Fig. 2a). A prominent feature of the summer precipitation signal is an East to West  
284 signature of increasing summer precipitation.

285 Our reconstruction shows a good match to Guiot and Kaniewski (2015) who have also discussed  
286 a possible east-to-west division in the Mediterranean with regard to precipitation (summer and  
287 annual) during the Holocene. They report wet centennial-scale spells in the eastern  
288 Mediterranean during the Early Holocene (until 6000 years BP), with dry spells in the western  
289 Mediterranean. Mid-Holocene reconstructions show continued wet conditions, with drying  
290 through the late Holocene (Guiot and Kaniewski, 2015). This pattern indicates a see-saw effect  
291 over the last 10,000 years, particularly during dry episodes in the Near and Middle East. As in  
292 our findings, Mauri et al. (2015) also reconstruct high annual precipitation values over much of  
293 the southern Mediterranean, and a weak winter precipitation signal. Mauri et al. (2015) confirm  
294 an east-west gradient for summer precipitation, with conditions drier or close to present in  
295 south-western Europe and wetter in the central and eastern Mediterranean (Fig 2b). These  
296 studies corroborate the hypothesis of an east-to-west division in precipitation during the early  
297 to mid-Holocene in the Mediterranean as proposed by Roberts et al. (2011). Roberts et al.  
298 (2011) suggest the eastern Mediterranean (mainly Turkey and more eastern regions)  
299 experienced higher winter precipitation during the early Holocene, followed by an oscillatory  
300 decline after 6000 yrs BP. Our findings reveal wetter annual and summer conditions in the  
301 eastern Mediterranean, although the winter precipitation signal is less clear. However, the



302 highest precipitation values reported by Roberts et al. (2011) were from sites located in western-  
303 central Turkey; these sites are absent in the current study. Climate variability in the eastern  
304 Mediterranean during the last 6000 years is documented in a number of studies based on  
305 multiple proxies (Finné et al., 2011). Most palaeoclimate proxies indicate wet mid-Holocene  
306 conditions (Bar-Matthews et al., 2003; Stevens et al., 2006; Eastwood et al., 2007; Kuhnt et al.,  
307 2008; Verheyden et al., 2008) which agree well with our results; however most proxies are not  
308 seasonally resolved.

309 Roberts et al. (2011) and Guiot and Kaniewski (2015) suggest that changes in precipitation in  
310 the western Mediterranean were smaller in magnitude during the early Holocene, while the  
311 largest increases occurred during the mid-Holocene, around 6000-3000 cal BP, before declining  
312 to modern values. Speleothems from southern Iberia suggests a humid early Holocene (9000-  
313 7300 cal BP) in southern Iberia, with equitable rainfall throughout the year (Walczak et al.,  
314 2015). Our reconstructions for the Alboran Sea which clearly shows an amplified precipitation  
315 seasonality (with higher annual/winter and lower than present summer rainfall) for the Alboran  
316 sites. It is likely that seasonal patterns defining the Mediterranean climate must have been even  
317 stronger in the early Holocene to support the wider development of sclerophyll forests than  
318 present in south Spain (Fletcher et al., 2013).

319

320 Late Holocene (4000 to 2000 cal yrs BP)

321 Annual precipitation reconstructions suggest drier or near-modern conditions in central Italy  
322 and Malta (Fig. 2b). In contrast, the Alboran and Aegean seas remain wetter. Winter and  
323 summer precipitation produce opposing patterns: a clear east-west division exists for summer  
324 precipitation, with a maximum in the eastern and a minimum over the western and central  
325 Mediterranean (Fig. 2b). Winter precipitation shows the opposite trend, with a maximum in the  
326 western Mediterranean and a minimum in the central and eastern Mediterranean (Fig. 2b). Our  
327 results are also in agreement with lakes and speleothem isotope records over the Mediterranean  
328 for the late Holocene (Roberts et al., 2011), and the Finné et al. (2011) palaeoclimate synthesis  
329 for the eastern Mediterranean. There is a good overall correspondence between trends and  
330 patterns in our reconstruction and that of Mauri et al. (2015), except for the Alboran Sea (Fig.  
331 2b). High-resolution speleothem data from southern Iberia show Mediterranean climate  
332 conditions in southern Iberia between 4800 and 3000 cal BP (Walczak et al., 2015) which is in  
333 agreement with our reconstruction. The Mediterranean climate conditions reconstructed here



334 for the Alboran Sea during the late Holocene is consistent with a climate reconstruction  
335 available from the Middle Atlas (Morocco), which show a trend over the last 6000 years  
336 towards arid conditions as well as higher precipitation seasonality between 4000 and 2000 cal  
337 yrs BP (Nourelbait et al., 2016). There is also good evidence from many records to support late  
338 Holocene aridification in southern Iberia. Paleoclimatic studies document a progressive  
339 aridification trend since ~7000 cal yr BP (e.g. Carrion et al., 2010; Jimenez-Moreno et al., 2015,  
340 Ramos-Roman et al., 2016), although a reconstruction of the annual precipitation inferred from  
341 pollen data with the Probability Density Function method indicate stable and dry conditions in  
342 the south of the Iberian Peninsula between 9000 and 3000 cal BP (Tarroso et al., 2016).

343 The current study shows that a prominent feature of late Holocene climate is the east-west  
344 division in precipitation, which varies based on the seasonal parameter reconstructed: summers  
345 were overall dry or near-modern in the central and western Mediterranean and wetter in the  
346 eastern Mediterranean, while winters were wet in the western Mediterranean and drier in the  
347 central and eastern Mediterranean.

348

#### 349 *Data-model comparison*

350 Figure 3 shows the data-model comparisons for the early to mid-Holocene (a) and late Holocene  
351 (b) compared to present values (in anomalies). Encouragingly, there is a good overall  
352 correspondence between patterns and trends in pollen-inferred precipitation and model outputs.  
353 Caution is required when interpreting climate model results as many of the changes depicted in  
354 Fig. 3 are very small and of marginal statistical significance, suggesting a high degree of  
355 uncertainty around their robustness.

356 For the early to mid-Holocene, both model and data indicate wet annual, winter and summer  
357 conditions in the Eastern Mediterranean. There are indications of an east to west division in  
358 summer precipitation simulated by the climate model (the magnitude of the increase in the  
359 eastern side of the basin is, however, extremely small). Furthermore, in the Aegean Sea, the  
360 model shows a good match with pollen-based reconstructions, suggesting that the increased  
361 spatial resolution of the regional climate model helps to simulate the localized, “patchy”,  
362 impacts of Holocene climate change, when compared to coarser global GCMs (Fig. 3). In Italy,  
363 the model shows a good match with pollen-based reconstructions with regards to the contrasting  
364 north-south precipitation regimes, but there is little agreement between model output and  
365 climate reconstruction with regard to winter and annual precipitation in southern Italy. The



366 climate model suggests wetter winter and annual conditions in the far western Mediterranean  
367 (i.e., western Iberia and the NW coast of Africa) – similar to pollen-based reconstructions – and  
368 near-modern summer conditions during summers.

369 Model and pollen-based reconstructions for the late Holocene indicate declining winter  
370 precipitation in the eastern Mediterranean and southern Italy (Sicily and Malta), although  
371 model-based changes are not statistically significant. In contrast, late Holocene summer  
372 precipitation is higher than today in the eastern Mediterranean (though only marginally so in  
373 the climate model). The east-west division in summer precipitation is strongest during the late  
374 Holocene and there are suggestions that it appears to be consistently simulated in the climate  
375 model but again, the signal – particularly in the Eastern Mediterranean – is not statistically  
376 significant.

377 Our findings are consistent with previous data-model comparisons based on the same regional  
378 model. Previous comparisons suggested that the winter precipitation signal was strongest in the  
379 northeastern Mediterranean (near Turkey) during the early Holocene (Brayshaw et al., 2011a;  
380 Roberts et al., 2011) and that there was a drying trend in the Mediterranean from the early  
381 Holocene to the late Holocene, particularly in the east. This is coupled with a gradually  
382 weakening seasonal cycle of surface air temperatures towards the present.

383 In contrast to Holocene winter precipitation changes in the Mediterranean (which are consistent  
384 with simulated changes in Mediterranean storm tracks; Brayshaw et al 2010), it is clear that  
385 most global climate models (PMIP2, PMIP3) simulate only very small changes in summer  
386 precipitation in the Mediterranean during the Holocene (Braconnot et al., 2007a,b, 2012; Mauri  
387 et al., 2014). The lack of a summer precipitation signal is consistent with the failure of the north-  
388 eastern extension of the west African monsoon to reach the southeastern Mediterranean, even  
389 in the early-to-mid-Holocene (Brayshaw et al., 2011a). Even though the regional climate model  
390 simulates a small change in precipitation compared to the proxy results, it cannot be robustly  
391 identified as statistically significant. This is to some extent unsurprising, insofar as the regional  
392 climate simulations presented here are themselves “driven” by data derived from a coarse global  
393 model (which, like its PMIP2/3 peers, does not simulate an extension of the African monsoon  
394 into the Mediterranean during this time period). Therefore, questions about summer  
395 precipitation in the Eastern Mediterranean during the Holocene remain. Climate dynamics need  
396 to be better understood in order to confidently reconcile proxy data (which suggest increased  
397 summer precipitation during the early Holocene in the Eastern Mediterranean) with climate  
398 model results. Based on the high-resolution coupled climate model EC-Earth, Bosmans et al.



399 (2015) shows how the seasonality of Mediterranean precipitation should vary from minimum  
400 to maximum precession, indicating a reduction in precipitation seasonality, due to changes in  
401 storm tracks and local cyclogenesis (*i.e.*, no direct monsoon required). Such high-resolution  
402 climate modeling studies (both global and regional) may prove a key ingredient in simulating  
403 the relevant atmospheric processes (both local and remote) and providing fine-grain spatial  
404 detail necessary to compare results to palaeo-proxy observations.

405 Future work based on transient Holocene model simulations are important, nevertheless,  
406 transient-model simulations have also shown mid-Holocene data-model discrepancies (Fischer  
407 and Jungclaus, 2011; Renssen et al., 2012). It is, however, suggested that further work is  
408 required to fully understand changes in winter and summer circulation patterns over the  
409 Mediterranean (Bosmans et al., 2015).

410

#### 411 *Limitations*

412 Classic ecological works for the Mediterranean (e.g. Ozenda 1975) highlight how precipitation  
413 limits vegetation type in plains and lowland areas, but temperature gradients take primary  
414 importance in mountain systems. Also, temperature and precipitation changes are not  
415 independent, but interact through bioclimatic moisture availability and growing season length  
416 (Prentice et al., 1996). This may be one reason why certain sites diverge from model outputs:  
417 the Alboran sites, for example, integrate pollen from the coastal plains through to mountain  
418 (+1500m) elevations. At high elevations within the source area, temperature effects become  
419 more important than precipitation in determining the forest cover type. So, it will not be possible  
420 to fully isolate precipitation signals from temperature changes. Particularly for the semiarid  
421 areas of the Mediterranean, the reconstruction approach probably cannot distinguish between a  
422 reduction in precipitation and an increase in temperature and PET, or vice versa.

423 Along similar lines, while the concept of reconstructing winter and summer precipitation  
424 separately is very attractive, it may be worth openly commenting on some limitations. Although  
425 different levels of the severity or length of summer drought are an important ecological  
426 limitation for vegetation, reconstructing absolute summer precipitation can be difficult as the  
427 severity/length of bioclimatic drought is determined by both temperature and precipitation.  
428 Also, we are dealing with a season which has, by definition, small amounts of precipitation that  
429 drop below the requirements for vegetation growth. Elevation is also of concern, as lowland  
430 systems tend to be recharged by winter rainfall, but high mountain systems may receive a





431 significant part of precipitation as snowfall, which is not directly available to plant life. This  
432 may be important in the long run for improving the interpretation of long-term Holocene  
433 changes and contrasts between different proxies, such as lake-levels and speleothems. All of  
434 these points may seem very picky on the ecology side, but they may have a real influence  
435 leading to problems and mismatches between different reconstruction approaches and different  
436 proxies (e.g. Davis et al., 2003; Mauri et al., 2015).

437 Another important point is the question of human impact on the Mediterranean vegetation  
438 during the Holocene. Since human activity has influenced natural vegetation, distinguishing  
439 between vegetation change induced by humans and climatic change in the Mediterranean is a  
440 challenge requiring independent proxies and approaches. Therefore links and processes behind  
441 societal change, and climate change in the Mediterranean region increasingly being investigated  
442 (eg. Holmgren et al., 2016; Gogou et al., 2016; Sadori et al., 2016a). Here, the behavior of the  
443 reconstructed climatic variables between 4000 and 2000 cal yrs BP is likely to be influenced  
444 by non-natural ecosystem changes due to human activities such as the forest degradation that  
445 began in lowlands, progressing to mountainous areas (Carrión et al., 2010). These human  
446 impacts add confounding effects for fossil pollen records and may lead to slightly biased  
447 temperature reconstructions during the Late Holocene, likely biased towards warmer  
448 temperatures and lower precipitation. However, if human activities become more marked at  
449 3000 cal ky BP, they increase significantly over the last millennia (Sadori et al., 2016) which  
450 is not within the time scale studied here. Moreover there is strong agreement between summer  
451 precipitation and independently reconstructed lake-level curves (Magny et al., 2013). For the  
452 marine pollen cores, human influence is much more difficult to interpret given that the source  
453 area is so large, and that, in general, anthropic taxa are not found in marine pollen assemblages.

454

## 455 **Conclusions**

456 The Mediterranean is particularly sensitive to climate change but the extent of future change  
457 relative to changes during the Holocene remains uncertain. Here, we present a reconstruction  
458 of Holocene precipitation in the Mediterranean using an approach based on both terrestrial and  
459 marine pollen records, along with a model-data comparison. We investigate climatic trends  
460 across the Mediterranean during the Holocene to test the hypothesis of an alternating north-  
461 south precipitation regime, and/or an east-west precipitation dipole. We give particular  
462 emphasis to the reconstruction of seasonal precipitation considering the important role it plays  
463 in this system.



464 Climatic trends reconstructed in this study seem to corroborate the north-south division of  
465 precipitation regimes during the Holocene, with wet conditions in the south-central and eastern  
466 Mediterranean, and dry conditions above 45°N during the early Holocene, while the opposite  
467 pattern dominates during the late Holocene. This study also shows that a prominent feature of  
468 Holocene climate in the Mediterranean is the east-to-west division in precipitation, strongly  
469 linked to the seasonal parameter reconstructed. During the early Holocene, we observe an east-  
470 to-west division with high summer precipitation in the central and eastern Mediterranean and a  
471 minimum over the western Mediterranean, while the signal for winter precipitation is less  
472 spatially consistent. There was a drying trend in the Mediterranean from the early Holocene to  
473 the late Holocene, particularly in central and eastern regions but summers in the east remained  
474 wetter than today.

475 The regional climate model outputs show a remarkable qualitative agreement with our pollen-  
476 based reconstructions, though it must be emphasised that the changes simulated are typically  
477 very small and of questionable statistical significance. Nevertheless, there are indications that  
478 the east to west division in summer precipitation reconstructed from the pollen records do  
479 appear to be simulated by the climate model. The model results also suggest that parts of the  
480 eastern Mediterranean experienced wetter conditions both in winter and in summer during the  
481 early and late Holocene and marginally wetter conditions in summer during the late Holocene  
482 (both consistent with the paleo-records). It is therefore noted that the use of higher-resolution  
483 climate models (both regional and global) may offer benefits for data-model comparison: both  
484 due to the inherently “patchy” nature of climate signals and palaeo-records, and through the  
485 better representation of the underlying atmospheric dynamics. It is therefore argued that more  
486 model simulations – ideally with higher resolution atmospheric dynamics – are required to fully  
487 understand the changes in the winter and summer circulation patterns over the Mediterranean  
488 region.

489

#### 490 **Acknowledgements**

491 This study is a part of the LAMA ANR Project (MSHE Ledoux, USR 3124, CNRS)  
492 financially supported by the French CNRS (National Centre for Scientific Research). Simon  
493 Goring is currently supported by NSF Macrosystems grant 144-PRJ45LP. This is an ISEM  
494 contribution n°XXXX.

495



496 **Figure captions**

497 Figure 1: Locations of terrestrial and marine pollen records along a longitudinal gradient from  
498 west to east and along a latitudinal gradient from northern Italy to Malta. Ombrothermic  
499 diagrams are shown for each site, calculated with the NewLoclim software program and  
500 database, which provides estimates of average climatic conditions at locations for which no  
501 observations are available (ex.: marine pollen cores).

502 Figure 2:

503 (a) Pollen-inferred climate estimates as performed with the Modern Analogues Technique  
504 (MAT): annual precipitation, winter precipitation (winter = sum of December, January  
505 and February precipitation) and summer precipitation (summer = sum of June, July  
506 and August precipitation). Changes in climate are expressed as differences with  
507 respect to the modern values (anomalies, mm/day). The modern values are derived  
508 from the ombrothermic diagrams (cf fig. 1). Two key intervals of the Holocene  
509 corresponding to the two time slice experiments (fig. 3) have been chosen: 8000–6000  
510 and 4000–2000 cal yrs BP. The climate values available during these periods have  
511 been averaged (stars).

512 (b) Comparison of our pollen-based climate reconstructions for the Mediterranean region with  
513 the pollen-inferred climate reconstruction at the European scale of Mauri et al (2015),  
514 expressed in anomaly (mm/month). These authors used the MAT with a modern  
515 analogue selection based on PFT (plant functional type) scores (and not pollen  
516 assemblages like the method used in this paper) and a 4D interpolation technique to  
517 produce gridded paleoclimate maps (for more details, see Mauri et al., 2015).

518 Figure 3: Data-model comparison for mid and late Holocene precipitation, expressed in  
519 anomaly (mm/day). Simulations are based on a regional model (Brayshaw et al., 2010):  
520 standard model HadAM3 coupled to HadSM3 (dynamical model) and HadRM3 (high-  
521 resolution regional model). The plots are hatched where it passes a significance test (threshold  
522 used here 70%). Pollen-inferred climate estimates (stars) are the same as in Figure 2: annual  
523 precipitation, winter precipitation (winter = sum of December, January and February  
524 precipitation) and summer precipitation (summer = sum of June, July and August  
525 precipitation).

526

527 Table 1: Metadata for the terrestrial and marine pollen records evaluated.

528



529 **References**

- 530 Alpert, P., Baldi, M., Ilani, R., Krichak, S., Price, C., Rodó, X., Saaroni, H., Ziv, B., Kishcha,  
531 P., Barkan, J., Mariotti, A. and Xoplaki, E.: Relations between climate variability in the  
532 Mediterranean region and the Tropics: ENSO, South Asian and African monsoons, hurricanes  
533 and Saharan dust In: Lionello P, Malanotte-Rizzoli P, Boscolo R (eds) Mediterranean  
534 Climate Variability, Amsterdam, Elsevier 149-177, 2006.
- 535 Bar-Matthews, M., Ayalon, A., Gilmour, M., Matthews, A. and Hawkesworth, C.J.: Sea-land  
536 oxygen isotopic relationships from planktonic foraminifera and speleothems in the Eastern  
537 Mediterranean region and their implication for paleorainfall during interglacial intervals.  
538 *Geochimica et Cosmochimica Acta* 67, 3181-3199, 2003.
- 539 Bar-Matthews, M. and Ayalon, A.: Mid-Holocene climate variations revealed by high-  
540 resolution speleothem records from Soreq Cave, Israel and their correlations with cultural  
541 changes, *Holocene*, 21, 163–172, 2011.
- 542 Bartlein, P.J., Harrison, S.P., Brewer, S., Connor, S., Davis, B.A.S., Gajewski, K., Guiot, J.,  
543 Harrison-Prentice, T.I., Henderson, A., Peyron, O., Prentice, I.C., Scholze, M., Seppä, H.,  
544 Shuman, B., Sugita, S., Thompson, R.S., Vial, A.E, Williams, J., and Wu H.: Pollen-based  
545 continental climate reconstructions at 6 and 21 ka: a global synthesis, *Climate Dynamics* 37,  
546 775-802, 2011.
- 547 Bosmans, J.H.C., Drijfhout, S.S., Tuenter, E., Hilgen, F.J., Lourens, L.J. and Rohling, E.J.:  
548 Precession and obliquity forcing of the freshwater budget over the Mediterranean, *Quaternary*  
549 *Science Reviews*, 123, 16-30, 2015.
- 550 Braconnot, P., Otto-Bliesner, B., Harrison, S., Joussaume, S., Peterchmitt, J.-Y., Abe-Ouchi,  
551 A., Crucifix, M., Driesschaert, E., Fichet, Th., Hewitt, C. D., Kageyama, M., Kitoh, A.,  
552 Laine, A., Loutre, M.-F., Marti, O., Merkel, U., Ramstein, G., Valdes, P., Weber, S. L., Yu,  
553 Y., and Zhao, Y.: Results of PMIP2 coupled simulations of the Mid-Holocene and Last  
554 Glacial Maximum –Part 1: experiments and large-scale features, *Clim. Past*, 3, 261–277,  
555 2007a.
- 556 Braconnot, P., Otto-Bliesner, B., Harrison, S., Joussaume, S., Peterchmitt, J.-Y., Abe-Ouchi,  
557 A., Crucifix, M., Driesschaert, E., Fichet, Th., Hewitt, C. D., Kageyama, M., Kitoh, A.,  
558 Loutre, M.-F., Marti, O., Merkel, U., Ramstein, G., Valdes, P., Weber, L., Yu, Y., and Zhao,  
559 Y.: Results of PMIP2 coupled simulations of the Mid-Holocene and Last Glacial Maximum



- 560 – Part 2: feedbacks with emphasis on the location of the ITCZ and mid- and high latitudes  
561 heat budget, *Clim. Past*, 3, 279–296, 2007b.
- 562 Braconnot, P., Harrison, S., Kageyama, M., Bartlein, J., Masson, V., Abe-Ouchi, A., Otto-  
563 Bliesner, B., and Zhao, Y.: Evaluation of climate models using palaeoclimatic data, *Nat.*  
564 *Clim. Change*, 2, 417-424, 2012.
- 565 Brayshaw, D.J., Hoskins, B. and Black, E.: Some physical drivers of changes in the winter  
566 storm tracks over the North Atlantic and Mediterranean during the Holocene. *Philosophical*  
567 *Transactions of the Royal Society A: Mathematical, Physical and Engineering Sciences*, 368,  
568 5185-5223, 2010.
- 569 Brayshaw, D.J., Rambeau, C.M.C., and Smith, S.J.: Changes in the Mediterranean climate  
570 during the Holocene: insights from global and regional climate modelling, *Holocene* 21, 15-  
571 31, 2011a.
- 572 Brayshaw, D.J., Black, E., Hoskins, B. and Slingo, J.: Past climates of the Middle East. In:  
573 Mithen, S. and Black, E. (eds.) *Water, Life and Civilisation: Climate, Environment and*  
574 *Society in the Jordan Valley*. International Hydrology Series. Cambridge University Press,  
575 Cambridge, pp. 25-50, 2011b
- 576 Carrión, J.S., Fernández, S., Jiménez-Moreno, G., Fauquette, S., Gil-Romera, G., González-  
577 Sampériz, P. and Finlayson, C.: The historical origins of aridity and vegetation degradation in  
578 southeastern Spain, *Journal of arid environments*, 74, 731-736, 2010.
- 579 Cheddadi, R., Yu, G., Guiot, J., Harrison, S.P., and Prentice, I.C.: The climate of Europe 6000  
580 years ago, *Climate Dynamics* 13, 1-9, 1997.
- 581 Colmenero-Hidalgo, E., Flores, J.-A., and Sierro, F.J. Biometry of *Emiliana huxleyi* and its  
582 biostratigraphic significance in the eastern north Atlantic Ocean and Western Mediterranean  
583 Sea in the last 20,000 years, *Marine Micropaleontology*, 46, 247-263, 2002.
- 584 Colombaroli, D., Vannièrè, B., Chapron, E., Magny, M., and Tinner, W. Fire–vegetation  
585 interactions during the Mesolithic–Neolithic transition at Lago dell’Accesa, Tuscany, Italy,  
586 *The Holocene*, 18, 679–692, 2008.
- 587 Combourieu-Nebout, N., Paterne, M., Turon, J.-L., and Siani, G.: A high-resolution record of  
588 the Last Deglaciation in the Central Mediterranean sea: palaeovegetation and  
589 palaeohydrological evolution, *Quaternary Sci. Rev.*, 17, 303–332, 1998.



- 590 Combourieu-Nebout, N., Londeix, L., Baudin, F., and Turon, J.L.: Quaternary marine and  
591 continental palaeoenvironments in the Western Mediterranean Sea (Leg 161, Site 976,  
592 Alboran Sea): Palynological evidences, Proceeding of the Ocean Drilling Project, scientific  
593 results, 161, 457-468, 1999.
- 594 Combourieu-Nebout, N., Turon, J.L., Zahn, R., Capotondi, L., Londeix, L., and Pahnke, K.:  
595 Enhanced aridity and atmospheric high pressure stability over the western Mediterranean  
596 during North Atlantic cold events of the past 50 000 years, *Geology*, 30, 863-866, 2002.
- 597 Combourieu-Nebout, N., Peyron, O., Dormoy, I., Desprat, S., Beaudouin, C., Kotthoff, U.,  
598 and Marret, F.: Rapid climatic variability in the west Mediterranean during the last 25 000  
599 years from high resolution pollen data, *Clim. Past*, 5, 503-521, 2009.
- 600 Combourieu-Nebout, N., Peyron, O., Bout-Roumazeilles, V., Goring, S., Dormoy, I.,  
601 Joannin, S., Sadori, L., Siani, G., and Magny, M.: Holocene vegetation and climate  
602 changes in central Mediterranean inferred from a high-resolution marine pollen record  
603 (Adriatic Sea), *Clim. Past* 9, 2023-2042, 2013.
- 604 Davis, B. A. S., Brewer, S., Stevenson, A. C., and Guiot, J.: The temperature of Europe  
605 during the Holocene reconstructed from pollen data, *Quaternary Sci. Rev.*, 22, 1701–1716,  
606 2003.
- 607 Davis, B. A. S. and Brewer, S.: Orbital forcing and role of the latitudinal insolation/  
608 temperature gradient, *Clim. Dynam.*, 32, 143-165, 2009.
- 609 De Santis V. and Caldara M. The 5.5–4.5 kyr climatic transition as recorded by the  
610 sedimentation pattern of coastal deposits of the Apulia region, southern Italy, Holocene, 2015
- 611 Desprat, S., Combourieu-Nebout, N., Essallami, L., Sicre, M. A., Dormoy, I., Peyron, O.,  
612 Siani, G., Bout Roumazeilles, V., and Turon, J. L.: Deglacial and Holocene vegetation  
613 and climatic changes in the southern Central Mediterranean from a direct land-sea  
614 correlation, *Clim. Past*, 9, 767–787, 2013.
- 615 Djamali, M., Gambin, B., Marriner, N., Andrieu-Ponel, V., Gambin, T., Gandouin, E.,  
616 Médail, F., Pavon, D., Ponel, P., and Morhange, C.: Vegetation dynamics during the early to  
617 mid-Holocene transition in NW Malta, human impact versus climatic forcing. *Vegetation  
618 History and Archaeobotany* 22, 367-380, 2013.
- 619 Dormoy, I., Peyron, O., Combourieu Nebout, N., Goring, S., Kotthoff, U., Magny, M, and  
620 Pross, J.: Terrestrial climate variability and seasonality changes in the Mediterranean region



- 621 between 15,000 and 4,000 years B.P. deduced from marine pollen records, *Clim. Past*, 5, 615-  
622 632, 2009.
- 623 Drescher-Schneider, R., de Beaulieu, J.L., Magny, M., Walter-Simonnet, A.V., Bossuet, G.,  
624 Millet, L. Brugiapaglia, E., and Drescher A.: Vegetation history, climate and human impact  
625 over the last 15 000 years at Lago dell'Accesa, *Veg. Hist. Archaeobot.*, 16, 279–299, 2007.
- 626 Eastwood, WJ., Leng, M., Roberts, N. and Davis B.: Holocene climate change in the eastern  
627 Mediterranean region: a comparison of stable isotope and pollen data from Lake Gölhisar,  
628 southwest Turkey, *J. Quaternary Science* 22, 327–341, 2007.
- 629 Finné, M., Holmgren, K., Sundqvist, H.S., Weiberg, E., and Lindblom, M.: Climate in the  
630 eastern Mediterranean, and adjacent regions, during the past 6000 years, *J. Archaeol. Sci.*, 38,  
631 3153-3173, 2011.
- 632 Fischer N., and Junglaus, J. H.: Evolution of the seasonal temperature cycle in a transient  
633 Holocene simulation: orbital forcing and sea-ice, *Clim. Past*, 7, 1139-1148, 2011.
- 634 Fletcher, W.J., and Sánchez Goñi, M.F.: Orbital- and sub-orbital-scale climate impacts on  
635 vegetation of the western Mediterranean basin over the last 48,000 yr, *Quat. Res.* 70, 451-464,  
636 2008.
- 637 Fletcher, W.J., Sanchez Goñi, M.F., Peyron, O., and Dormoy, I.: Abrupt climate changes of  
638 the last deglaciation detected in a western Mediterranean forest record. *Clim. Past* 6, 245-264,  
639 2010.
- 640 Fletcher, W.J., Debret, M., and Sanchez Goñi, M.F., Mid-Holocene emergence of a low-  
641 frequency millennial oscillation in western Mediterranean climate: Implications for past  
642 dynamics of the North Atlantic atmospheric westerlies. *The Holocene*, 23, 153-166, 2013.
- 643 Gambin B., Andrieu-Ponel V., Médail F., Marriner N., Peyron O., Montade V., Gambin T.,  
644 Morhange C., Belkacem D., and Djamali M.: 7300 years of vegetation history and  
645 quantitative climate reconstruction for NW Malta: a Holocene perspective. *Clim. Past* 12,  
646 273-297, 2016
- 647 Geraga, M., Ioakim, C., Lykousis, V., Tsaila-Monopolis, S., and Mylona, G.: The high-  
648 resolution palaeoclimatic and palaeoceanographic history of the last 24,000 years in the  
649 central Aegean Sea, Greece, *Palaeogeogr. Palaeoclimatol.*, 287, 101–115, 2010.
- 650 Giorgi, F. and Lionello, P.: Climate change projections for the Mediterranean region, *Global*  
651 *Planet. Change*, 63, 90–104, 2008.



- 652 Gogou, A., Bouloubassi, I., Lykousis, V., Arnaboldi, M., Gaitani, P., and Meyers, P.A.:  
653 Organic geochemical evidence of abrupt late glacial- Holocene climate changes in the North  
654 Aegean Sea, *Palaeogeogr. Palaeoclimatol.*, 256, 1 – 20, 2007.
- 655 Gogou, A., Triantaphyllou, M., Xoplaki, E., Izdebski, A., Parinos, C., Dimiza, M.,  
656 Bouloubassi, I., Luterbacher, J., Kouli, K., Martrat, B., Toreti, A., Fleitmann, D., Rousakis,  
657 G., Kaberi, H., Athanasiou, M., and Lykousis, V.: Climate variability and socio-  
658 environmental changes in the northern Aegean (NE Mediterranean) during the last 1500  
659 years, *Quaternary Science Reviews*, 136, 209-228, 2016.
- 660 Guiot J.: Methodology of the last climatic cycle reconstruction in France from pollen data,  
661 *Palaeogeography, Palaeoclimatology, Palaeoecology*, 80, 49–69, 1990.
- 662 Guiot, J. and Kaniewski, D.: The Mediterranean Basin and Southern Europe in a warmer  
663 world: what can we learn from the past? *Front. Earth Sci.*, 18, 2015.
- 664 Hargreaves, J.C., Annan, J.D., Ohgaito, R., Paul, A., and Abe-Ouchi, A.: Skill and reliability  
665 of climate model ensembles at the Last Glacial Maximum and mid-Holocene, *Clim. Past*, 9,  
666 811-823, 2013.
- 667 Heiri, O., Brooks, S.J., Renssen, H., and 26 authors: Validation of climate model-inferred  
668 regional temperature change for late-glacial Europe. *Nature Communications* 5, 4914, 2014.
- 669 Heusser, L.E., and Balsam W.L.: Pollen distribution in the N.E. Pacific ocean, *Quaternary*  
670 *Research*, 7, 45-62, 1977.
- 671 Hewitt, C.D., Senior, C.A., and Mitchell, J.F.B. :The impact of dynamic sea-ice on the  
672 climatology and sensitivity of a GCM: A study of past, present and future climates, *Climate*  
673 *Dynamics* 17: 655–668, 2001.
- 674 Holmgren, K., Gogou, A., Izdebski, A., Luterbacher, J., Sicre, M.A., and Xoplaki, A.:  
675 Mediterranean Holocene Climate, Environment and Human Societies, *Quaternary Science*  
676 *Reviews*, 136, 1-4, 2016.
- 677 Ioakim, Chr., Triantaphyllou, M., Tsaila-Monopolis, S., and Lykousis, V.: New  
678 micropalaeontological records of Eastern Mediterranean marine sequences recovered offshore  
679 of Crete, during HERMES cruise and their palaeoclimatic paleoceanographic significance.  
680 *Acta Naturalia de “L’Ateneo Parmense”*, 45(1/4): p. 152. In: *Earth System Evolution and the*  
681 *Mediterranean Area from 23 Ma to the Present*”, 2009.





- 682 Jimenez-Moreno, G., Rodriguez-Ramirez, A., Perez-Asensio, J.N., Carrion, J.S., Lopez-  
683 Saez, J.A., Villarías-Robles J., Celestino-Perez, S., Cerrillo-Cuenca, E., Leon, A., and  
684 Contreras, C.: Impact of late-Holocene aridification trend, climate variability and geodynamic  
685 control on the environment from a coastal area in SW Spain, *The Holocene*, 1-11, 2015
- 686 Joannin, S., Vannière, B., Galop, D., Peyron, O., Haas, J.N., Gilli, A., Chapron, E., Wirth, S.,  
687 Anselmetti, F., Desmet, M., and Magny, M.: Climate and vegetation changes during the  
688 Lateglacial and Early-Mid Holocene at Lake Ledro (southern Alps, Italy), *Clim. Past* 9, 913-  
689 933, 2013.
- 690 Joannin, S., Brugiapaglia, E., de Beaulieu, J.L, Bernardo, L., Magny, M., Peyron, O., Goring,  
691 S., and Vannière, B.: Pollen-based reconstruction of Holocene vegetation and climate in  
692 southern Italy: the case of Lago Trifoglietti., *Clim. Past*, 8, 1973-1996, 2012.
- 693 Kotthoff, U., Pross, J., Müller, U.C., Peyron, O., Schmiedl, G., and Schulz, H. Climate  
694 dynamics in the borderlands of the Aegean Sea during formation of Sapropel S1 deduced  
695 from a marine pollen record, *Quaternary Sci. Rev.*, 27, 832–845, 2008.
- 696 Kotthoff, U., Koutsodendris, A., Pross, J., Schmiedl, G., Bornemann, A., Kaul, C., Marino,  
697 G., Peyron, O., and Schiebel, R. Impact of late glacial cold events on the Northern Aegean  
698 region reconstructed from marine and terrestrial proxy data, *J. Quat. Sci.*, 26, 86-96, 2011.
- 699 Kouli, K., Gogou, A., Bouloubassi, I., Triantaphyllou, M.V., Ioakim, Chr, Katsouras, G.,  
700 Roussakis, G., and Lykousis, V.: Late postglacial paleoenvironmental change in the  
701 northeastern Mediterranean region: Combined palynological and molecular biomarker  
702 evidence, *Quatern. Int.*, 261, 118-127, 2012.
- 703 Kuhnt, T., Schmiedl, G., Ehrmann, W., Hamann, Y., and Andersen, N.: Stable isotopic  
704 composition of Holocene benthic foraminifers from the eastern Mediterranean sea: past  
705 changes in productivity and deep water oxygenation. *Palaeogeography, Palaeoclimatology,*  
706 *Palaeoecology* 268, 106-115, 2008.
- 707 Lionello, P, Malanotte-Rizzoli, P, Boscolo, R, Alpert, P, Artale, V, Li, L. et al., The  
708 Mediterranean climate: An overview of the main characteristics and issues. In: Lionello P,  
709 Malanotte-Rizzoli P and Boscolo R (eds) *Mediterranean Climate Variability. Developments*  
710 *in Earth & Environmental Sciences* 4, Elsevier, 1–26, 2006.
- 711 Lionello, P. (Ed.): *The climate of the Mediterranean region, From the past to the future,*  
712 Elsevier, ISBN: 9780124160422, 2012.



- 713 Luterbacher, J., García-Herrera, R., Akcer-On, S., Allan R., Alvarez-Castro M.C. and 41  
714 authors: A review of 2000 years of paleoclimatic evidence in the Mediterranean. In: Lionello,  
715 P. (Ed.), *The Climate of the Mediterranean region: from the past to the future*. Elsevier,  
716 Amsterdam, The Netherlands, 2012.
- 717 Magny, M., de Beaulieu, J.L., Drescher-Schneider, R., Vannière, B., Walter-Simonnet, A.V.,  
718 Miras, Y., Millet, L., Bossuet, G., Peyron, O., Brugiapaglia, E., and Leroux, A. : Holocene  
719 climate changes in the central Mediterranean as recorded by lake-level fluctuations at Lake  
720 Accessa (Tuscany, Italy), *Quaternary Sci. Rev.* 26, 1736–1758, 2007.
- 721 Magny, M., Vannière, B., Zanchetta, G., Fouache, E., Touchais, G., Petrika, L., Coussot, C.,  
722 Walter-Simonnet, A.V., and Arnaud, F.: Possible complexity of the climatic event around  
723 4300-3800 cal BP in the central and western Mediterranean, *The Holocene*, 19, 823-833,  
724 2009.
- 725 Magny, M., Vannière, B., Calo, C., Millet, L., Leroux, A., Peyron, O., Zanchetta, G., La  
726 Mantia, T. and Tinner, W.: Holocene hydrological changes in south-western Mediterranean as  
727 recorded by lake-level fluctuations at Lago Preola, a coastal lake in southern Sicily, Italy,  
728 *Quaternary Sci. Rev.*, 30, 2459-2475, 2011.
- 729 Magny, M., Joannin, S., Galop, D., Vannière, B., Haas, J.N, Bassetti, M., Bellintani, P.,  
730 Scandolari, R., and Desmet, M.: Holocene palaeohydrological changes in the northern  
731 Mediterranean borderlands as reflected by the lake-level record of Lake Ledro, northeastern  
732 Italy, *Quaternary Res.*, 77, 382-396, 2012a.
- 733 Magny, M., Peyron, O., Sadori, L., Ortu, E., Zanchetta, G., Vannière, B., and Tinner, W.:  
734 Contrasting patterns of precipitation seasonality during the Holocene in the south- and north-  
735 central Mediterranean, *J. Quaternary Sci.*, 27, 290–296, 2012b.
- 736 Magny, M. and 29 authors: North-south palaeohydrological contrasts in the central  
737 Mediterranean during the Holocene: tentative synthesis and working hypotheses, *Clim. Past* 9,  
738 2043-2071, 2013.
- 739 Mauri, A., Davis, B., Collins, P.M. and Kaplan, J.: The climate of Europe during the  
740 Holocene: a gridded pollen-based reconstruction and its multi-proxy evaluation, *Quat. Sc.*  
741 *Rev.* 112, 109-127, 2014.



- 742 Mauri, A., Davis, B., Collins, P.M. and Kaplan, J.: The influence of atmospheric circulation  
743 on the mid-Holocene climate of Europe: a data–model comparison, *Clim. Past* 10, 1925-1938,  
744 2015.
- 745 Morrill, C., Anderson, D.M, Bauer, B.A, Buckner, R.E., Gille, P., Gross, W.S., Hartman, M.,  
746 and Shah, A.: Proxy benchmarks for intercomparison of 8.2 ka simulations, *Clim. Past* 9, 423-  
747 432, 2013.
- 748 Naughton, F., Sanchez Goñi, M.F., Desprat, S., Turon, J.L., Duprat, J., Malaizé, B., Joli, C.,  
749 Cortijo, E., Drago, T., and Freitas, M.C.: Present-day and past (last 25 000 years) marine  
750 pollen signal off western Iberia, *Marine Micropaleontology* 62, 91-114, 2007.
- 751 Nourelbait, M., Rhoujjati, A., Benkaddour, A., Carré, M., Eynaud, F., Martinez, P. and  
752 Cheddadi, R.: Climate change and ecosystems dynamics over the last 6000 years in the  
753 Middle Atlas, Morocco, *Clim. Past* 12, 1029-1042, 2016.
- 754 Peyron, O., Goring, S., Dormoy, I., Kotthoff, U., Pross, J., de Bealieu, J.L., Drescher-  
755 Schneider, R., and Magny, M.: Holocene seasonality changes in the central Mediterranean  
756 region reconstructed from the pollen sequences of Lake Accessa (Italy) and Tenaghi Philippon  
757 (Greece), *The Holocene*, 21, 131-146, 2011.
- 758 Peyron, O., Magny, M., Goring, S., Joannin, S., de Beaulieu, J.-L., Brugiapaglia, E., Sadori,  
759 L., Garfi, G., Kouli, K., Ioakim, C., and Combourieu-Nebout, N. Contrasting patterns of  
760 climatic changes during the Holocene in the central Mediterranean (Italy) reconstructed from  
761 pollen data, *Clim. Past* 9, 1233-2013, 2013.
- 762 Pope, V.D., Gallani, M.L., Rowntree, R.R. and Stratton, R.A.: The impact of new physical  
763 parameterizations in the Hadley Centre climate model: HadAM3, *Climate Dynamics* 16, 123-  
764 146, 2000.
- 765 Pross, J., Kotthoff, U., Müller, U.C., Peyron, O., Dormoy, I., Schmiedl, G., Kalaitzidis, S.,  
766 and Smith, A.M.: Massive perturbation in terrestrial ecosystems of the Eastern Mediterranean  
767 region associated with the 8.2 kyr climatic event, *Geology*, 37, 887-890, 2009.
- 768 Ramos-Román, M.J., Jiménez-Moreno, G., Anderson, R.S., García-Alix, A., Toney, J.L.,  
769 Jiménez-Espejo, F.J. and Carrión, J.S.: Centennial-scale vegetation and North Atlantic  
770 Oscillation changes during the Late Holocene in the southern Iberia, *Quaternary Science*  
771 *Reviews*, 143, 84-98, 2016.



- 772 Renssen, H., Seppa, H., Crosta, X., Goosse, H., and Roche, D.M.: Global characterization of  
773 the Holocene Thermal Maximum, *Quat. Sci. Rev.*, 48, 7-19, 2012.
- 774 Roberts, N., Brayshaw, D., Kuzucuoğlu, C., Perez, R., and Sadori, L.: The mid-Holocene  
775 climatic transition in the Mediterranean: Causes and consequences, *The Holocene*, 21, 3-13,  
776 2011.
- 777 Roberts, N., Moreno, A., Valero-Garces, B. L., Corella, J. P., Jones, M., Allcock, S., et al.  
778 Palaeolimnological evidence for an east-west climate see-saw in the mediterranean since AD  
779 900, *Glob. Planet. Change*, 84-85, 23-34, 2012.
- 780 Rohling, E.J., Cane, T.R., Cooke, S., Sprovieri, M., Bouloubassi, I., Emeis, K.C. et al: African  
781 monsoon variability during the previous interglacial maximum, *Earth Planet. Sc. Lett.*, 202,  
782 61-75, 2002.
- 783 Sadori, L. and Narcisi, B.: The postglacial record of environmental history from Lago di  
784 Pergusa, Sicily, *The Holocene*, 11, 655-671, 2001.
- 785 Sadori, L. and Giardini, M.: Charcoal analysis, a method to study vegetation and climate of  
786 the Holocene: The case of Lago di Pergusa, Sicily (Italy), *Geobios-Lyon*, 40, 173-180, 2007.
- 787 Sadori, L., Zanchetta, G., and Giardini, M.: Last Glacial to Holocene palaeoenvironmental  
788 evolution at Lago di Pergusa (Sicily, Southern Italy) as inferred by pollen, microcharcoal, and  
789 stable isotopes, *Quatern. Int.*, 181, 4-14, 2008.
- 790 Sadori, L., Jahns, S., and Peyron, O.: Mid-Holocene vegetation history of the central  
791 Mediterranean, *The Holocene*, 21, 117-129, 2011.
- 792 Sadori, L., Ortu, E., Peyron, O., Zanchetta, G., Vanni ere, B., Desmet, M., and Magny, M.: The  
793 last 7 millennia of vegetation and climate changes at Lago di Pergusa (central Sicily, Italy),  
794 *Clim. Past*, 9, 1969-1984, 2013.
- 795 Sadori, L., Giraudi, C. Masi, A., Magny, M., Ortu, E., Zanchetta, G., and Izdebski, A.  
796 Climate, environment and society in southern Italy during the last 2000 years. A review of the  
797 environmental, historical and archaeological evidence, *Quaternary Science Reviews*, 136,  
798 173-188, 2016a.
- 799 Sadori, L., Koutsodendris, A., Masi, A., Bertini, A., Combourieu-Nebout, N., Francke, A.,  
800 Kouli, K., Joannin, S., Mercuri, A.M, Panagiotopoulos, K., Peyron, O., Torri, P., Wagner, B.,  
801 Zanchetta, G., and Donders, T.H.: Pollen-based paleoenvironmental and paleoclimatic



- 802 change at Lake Ohrid (SE Europe) during the past 500 ka, *Biogeosciences* 12, 15461-15493,  
803 2016b.
- 804 Stevens, L.R., Ito, E., Schwalb, A., and Wright, H.E.: Timing of atmospheric precipitation in  
805 the Zagros Mountains inferred from a multi-proxy record from Lake Mirabad, Iran. *Quat.*  
806 *Res.* 66, 494-500, 2006.
- 807 Tarroso, P., Carrión, J., Dorado-Valiño, M., Queiroz, P., Santos, L., Valdeolmillos-Rodríguez,  
808 A., Célio Alves, P., Brito, J. C., and Cheddadi, R.: Spatial climate dynamics in the Iberian  
809 Peninsula since 15 000 yr BP, *Clim. Past*, 12, 1137-1149, 2016.
- 810 Triantaphyllou, V., Antonarakou, A., Kouli, K., Dimiza, M., Kontakiotis, G., Papanikolaou,  
811 M.D. et al.: Late Glacial–Holocene ecostratigraphy of the south-eastern Aegean Sea, based on  
812 plankton and pollen assemblages, *Geo-Mar. Lett.*, 29, 249-267, 2009a.
- 813 Triantaphyllou, M.V., Ziveri, P., Gogou, A., Marino, G., Lykousis, V., Bouloubassi, I.,  
814 Emeis, K.-C., Kouli, K., Dimiza, M., Rosell-Mele, A., Papanikolaou, M., Katsouras, G., and  
815 Nunez, N.: Late Glacial-Holocene climate variability at the south-eastern margin of the  
816 Aegean Sea, *Mar. Geol.*, 266, 182-197, 2009b.
- 817 Triantaphyllou, M.V., Gogou, A., Bouloubassi, I., Dimiza, M., Kouli, K., Rousakis, A.G.,  
818 Kotthoff, U., Emeis, K.C., Papanikolaou, M., Athanasiou, M., Parinos, C., Ioakim, C., V. and  
819 Lykousis, V.: Evidence for a warm and humid Mid-Holocene episode in the Aegean and  
820 northern Levantine Seas (Greece, NE Mediterranean), *Regional Environmental Change*, 14,  
821 1697-1712, 2014.
- 822 Triantaphyllou, M.V., Gogou, A., Dimiza, M.D., Kostopoulou, S., Parinos, C., Roussakis, G.,  
823 Geraga, M., Bouloubassi, I., Fleitmann, D., Zervakis, V., Velaoras, D., Diamantopoulou, A.,  
824 Sampataki, A. and Lykousis, V.: Holocene Climate Optimum centennial-scale  
825 paleoceanography in the NE Aegean Sea (Mediterranean Sea). *Geo-Marine Letters*, 36, 51-66,  
826 2016.
- 827 Trigo R.M. and 21 coauthors: Relations between variability in the Mediterranean region and  
828 Mid-latitude variability. In: Lionello P, Malanotte-Rizzoli P, Boscolo R, Eds., *The*  
829 *Mediterranean Climate: an overview of the main characteristics and issues.* Elsevier,  
830 Amsterdam, 2006.
- 831 Tzedakis, P.C.: Seven ambiguities in the Mediterranean palaeoenvironmental narrative,  
832 *Quaternary Sci. Rev.*, 26, 2042-2066, 2007.



- 833 Vanni re, B., Power, M.J., Roberts, N., Tinner, W., Carrion, J., Magny, M., Bartlein, P., and  
834 Contributors Data: Circum-Mediterranean fire activity and climate changes during the mid  
835 Holocene environmental transition (8500-2500 cal yr BP), *The Holocene*, 21, 53-73, 2011.
- 836 Vanni re, B., Magny, M., Joannin, S., Simonneau, A., Wirth, S.B., Hamann, Y., Chapron,  
837 E., Gilli, A., Desmet, M., and Anselmetti, F.S.: Orbital changes, variation in solar activity and  
838 increased anthropogenic activities: controls on the Holocene flood frequency in the Lake  
839 Ledro area, Northern Italy, *Clim. Past*, 9, 1193-1209, 2013.
- 840 Verheyden S., Nader F.H., Cheng H.J., Edwards L.R. and Swennen R.: Paleoclimate  
841 reconstruction in the Levant region from the geochemistry of a Holocene stalagmite from the  
842 Jeita cave, Lebanon. *Quaternary Research*, 70, 368-381, 2008.
- 843 Walczak, I.W., Baldini, J.U.L., Baldini, L.M., Mcdermott, F., Marsden, S., Standish, C.D,  
844 Richards, D.A., Andreo, B and Slater J.: Reconstructing high-resolution climate using CT  
845 scanning of unsectioned stalagmites: A case study identifying the mid-Holocene onset of the  
846 Mediterranean climate in southern Iberia, *Quaternary Science Reviews* 127, 117-128, 2015.
- 847 Wilks D. S.: *Statistical methods in the atmospheric sciences* (Academic Press, San Diego,  
848 CA), 1995.
- 849 Wood, S.N. Fast stable restricted maximum likelihood and marginal likelihood estimation of  
850 semiparametric generalized linear models. *Journal of the Royal Statistical Society (B)* 73(1),  
851 3-36, 2011.
- 852 Wu, H., Guiot, J., Brewer, S., and Guo, Z.: Climatic changes in Eurasia and Africa  
853 at the Last Glacial Maximum and mid-Holocene: reconstruction from pollen data using  
854 inverse vegetation modelling, *Clim. Dyn.*, 29, 211-229, 2007.
- 855 Zanchetta, G., Borghini, A., Fallick, A.E., Bonadonna, F.P., and Leone, G.: Late Quaternary  
856 palaeohydrology of Lake Pergusa (Sicily, southern Italy) as inferred by stable isotopes of  
857 lacustrine carbonates, *J. Paleolimnol.*, 38, 227-239, 2007.
- 858 Zhornyak, L.V., Zanchetta, G., Drysdale, R.N., Hellstrom, J.C., Isola, I., Regattieri, E.,  
859 Piccini, L., Baneschi, I., and Couchoud, I.: Stratigraphic evidence for a “pluvial phase”  
860 between ca. 8200-7100 ka from Renella cave (Central Italy), *Quat. Sci. Rev.*, 30, 409-417,  
861 2011.

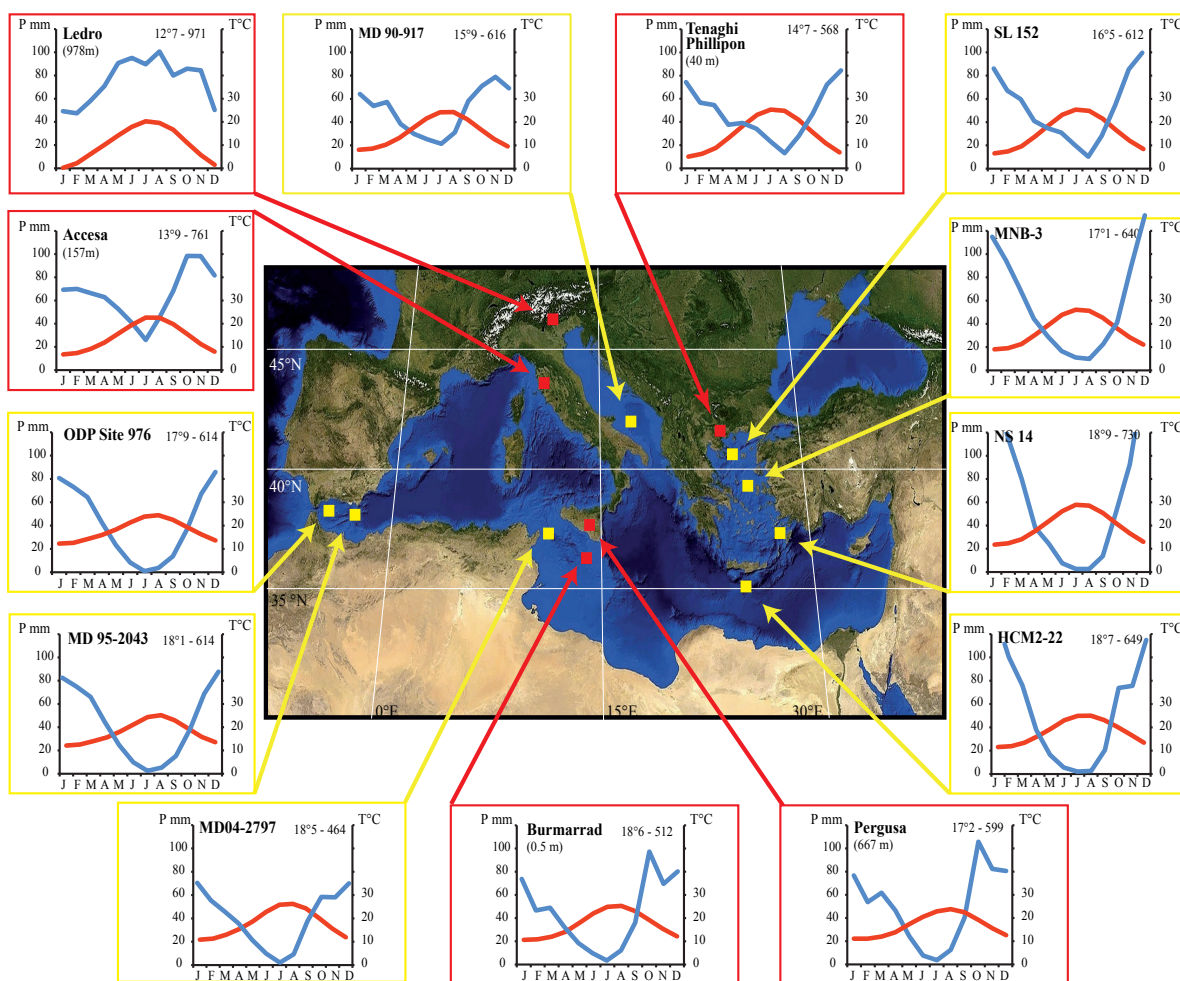


Figure 1: Locations of terrestrial (red) and marine (yellow) pollen records. Ombrothermic diagrams are calculated with the NewLoclim software, which provides estimates of average climatic conditions at locations for which no observations are available (ex.: marine pollen cores).

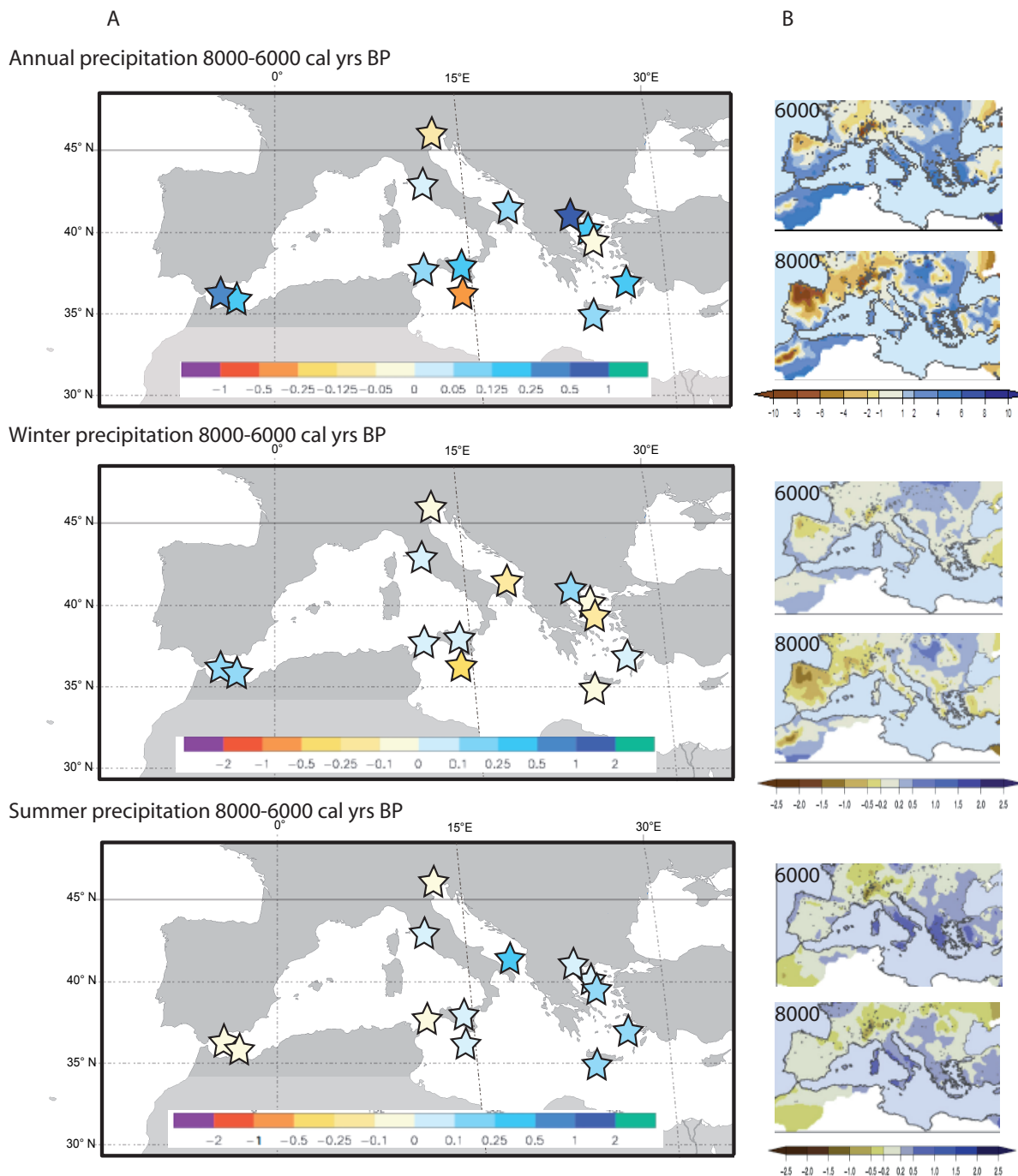


Figure 2: 8000-6000 cal years BP  
 (A) Pollen-inferred climate estimates as performed with the Modern Analogues Technique : annual precipitation, winter precipitation (winter = sum of December, January and February precipitation) and summer precipitation (summer = sum of June, July and August precipitation). Changes in climate are expressed as differences with respect to the modern values (anomalies, mm/day) which are derived from the ombrothermic diagrams (cf fig. 1). Climate values reconstructed during the 8000-6000 cal yrs BP have been averaged (stars).  
 (B) Pollen-inferred climate reconstruction at the European scale of Mauri et al (2015), expressed in anomaly (mm/month). These authors used a modern analogue selection based on PFT (plant functional type) scores (and not pollen assemblages like the method used in A) and a 4D interpolation technique to produce gridded paleoclimate maps (for more details, see Mauri et al., 2015).



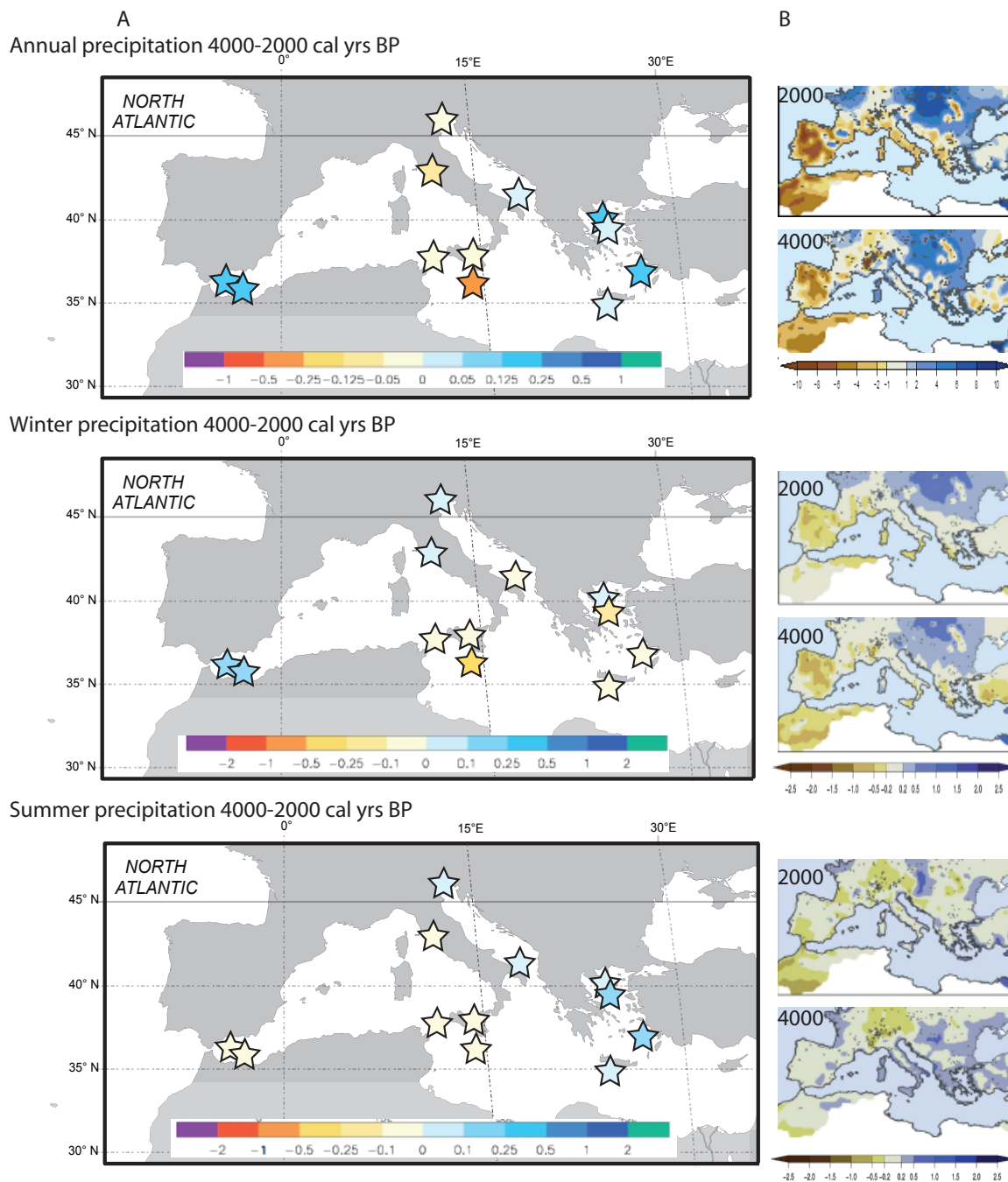
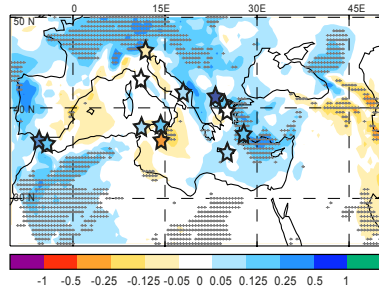


Figure 2: 4000-2000 cal yrs BP

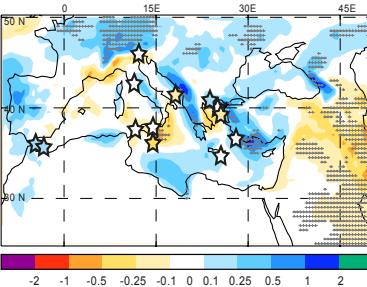


### Mid-Holocene: 8000 to 6000 cal BP

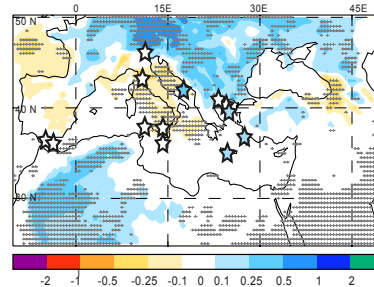
(a) Annual precipitation (anomalie mm/day)



(b) winter precipitation (anomalie mm/day)



(c) summer precipitation (anomalie mm/day)



### Late Holocene: 4000 to 2000 cal BP

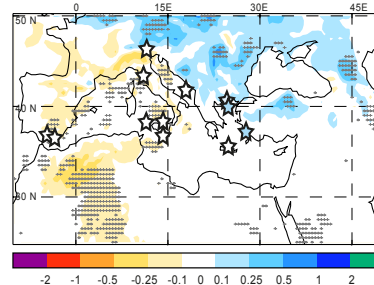
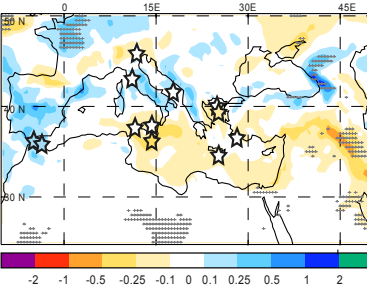
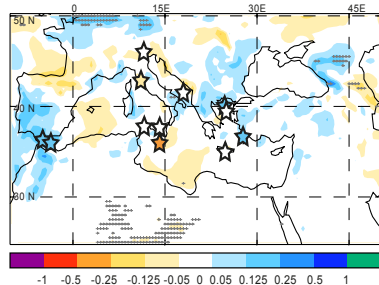


Figure 3: Data-model comparison for mid and late Holocene precipitation, expressed in anomaly (mm/day).

Simulations are based on a regional model (Brayshaw et al., 2010): standard model HadAM3 coupled to HadSM3 (dynamical model) and HadRM3 (high-resolution regional model). The plots are hatched where it passes a significance test (threshold used here 70%).

Pollen-inferred climate estimates (stars) are the same as in Figure 2: annual precipitation, winter precipitation and summer precipitation .



| <b>Terrestrial pollen records</b>         |                  |                 |                                 |  |
|---|------------------|-----------------|---------------------------------|--|
|   | <b>Longitude</b> | <b>Latitude</b> | <b>Elevation<br/>(m a.s.l.)</b> | <b>References</b>  |
| <b>Lago di Ledro</b> (Northern Italy)     | 10°76'E          | 45°87'N         | 652                             | Joannin et al. (2013), Magny et al. (2009, 2012a), Vanni re et al. (2013), Peyron et al. (2013)  |
| <b>Accesa</b> (Central Italy)             | 10°53'E          | 42°59'N         | 157                             | Drescher-Schneider et al. (2007), Magny et al. (2007, 2013), Colombaroli et al. (2008), Sadori et al. (2011), Vanni re et al. (2011), Peyron et al. (2011, 2013) |
| <b>Trifoglietti</b> (southern Italy)      | 16°01'E          | 39°33'N         | 1048                            | Joannin et al., (2012) ;<br>Peyron et al. (2013)   |
| <b>Pergusa</b> (Sicily)                   | 14°18'E          | 37°31'N         | 667                             | Sadori and Narcisi (2001); Sadori and Giardini (2007); Sadori et al. (2008, 2011, 2013, 2016b); Magny et al. (2011, 2013)  |
| <b>Tenaghi Philippon</b> (Greece)         | 24°13.4'E        | 40°58.4'N       | 40                              | Pross et al., (2009, 2015); Peyron et al. (2011); Schemmel et al., (2016)  |
| <b>Burmarrad</b> (Malta)                  | 14°25'E          | 35°56'N         | 0.5                             | Djamali et al., (2013); Gambin et al., (2016)  |
| <b>Marine pollen records</b>              |                  |                 |                                 |  |
|   | <b>Longitude</b> | <b>Latitude</b> | <b>Water-<br/>depth</b>         | <b>References</b>  |
| <b>ODP 976</b> (Alboran Sea)              | 4°18'W           | 36°12' N        | 1108                            | Combourieu-Nebout et al., (1999, 2002, 2009) ; Dormoy et al., (2009)   |
| <b>MD95-2043</b> (Alboran Sea)            | 2°37'W           | 36°9'N          | 1841                            | Fletcher and S nchez Go ni( 2008); Fletcher et al., (2010)   |
| <b>MD90-917</b> (Adriatic Sea)            | 17°37'E          | 41°97'N         | 845                             | Combourieu-Nebout et al., (2013)   |
| <b>MD04-2797</b> (Siculo-Tunisian strait) | 11°40'E          | 36°57'N         | 771                             | Desprat et al., (2013)   |
| <b>SL152</b> (North Aegean Sea)           | 24°36' E         | 40°19' N        | 978                             | Kotthoff et al., (2008, 2011), Dormoy et al., (2009).  |
| <b>NS14</b> (South Aegean Sea)            | 27°02.87'E       | 36°38.9'N       | 505                             | Kouli et al., (2012) ; Gogou et al., (2007); Triantaphyllou et al., (2009a, b)   |
| <b>HCM2/22</b> (south Crete)              | 24°53'E          | 34°34 N         | 2211                            | Kouli et al., (2012) ; Triantaphyllou et al., (2014)   |
| <b>MNB-3</b> (North Aegean Sea)           | 25°00'E          | 39°15.43'N      | 800                             | Kouli et al., (2012) ; Triantaphyllou et al., (2014)   |

Table 1: Metadata for the terrestrial and marine pollen records evaluated.